AD-A277 372

ITATION PAGE Approved for public release; distribution unlimited. Form Approved OMB No. 0704-0188

Public reporting burden for this collection of information is estimated to average ... hour per response, including the time for reviewing instructions, searching existing data sources, gathering and maintaining the data needed, and completing and reviewing the collection of information. Send comments regarding this burden estimate or any other aspect of this collection of information, including suggestions for reducing this burden, to Washington Headquarters Services, Directorate for information Operations and Reports, 1215 Jefferson Davis Highway, Suite 1204, Arlington, VA 22202-4302, and to the Office of Management and Budget, Paperwork Reduction Project (0704-0188), Washington, DC 20503.

T DATE	3. REPORT TYPE AND DATES COVERED
28 January 1994	Final 1 December 1990 - 30 November 1993

4. TITLE AND SUBTITLE

Time-resolved IR spectroscopy, energy transfer, and state-to-state collision dynamics of atmospheric species

5. FUNDING NUMBERS

AFOSR90-0055

Task # 2303/ES

6. AUTHOR(S)

David J. Nesbitt

7. PERFORMING ORGANIZATION NAME(S) AND ADDRESS(ES)

University of Colorado
Boulder, CO 80309-0019

8. PERFORMING ORGANIZATION REPORT NUMBER

AFOSR-TR- 94 0057

9. SPONSORING MONITORING AGENCY NAME(S) AND ADDRESS(ES)

AFOSR/NC
Building 410
Bolling AFB DC
20332-6448

DTIC ELECTE MAR 23 1994 S B D

10. SPONSORING MONITORING

94-09110

11. SUPPLEMENTARY NOTES

12a. DISTRIBUTION AVAILABILITY STATEMENT

Approved for public release;
distribution is unlimited

12b. DISTRIBUTION CODE

13. ABSTRACT *(Maximum 200 words)*

Achievements under the AFOSR grant have been in the following areas 1) We have developed a new method for state-to-state collisional energy transfer in crossed molecular beams, based on high sensitivity direct IR laser absorption, and allowing absolute cross sections to be obtained by measurement of absolute number densities of the scattering species (CH_4, H_2O, HF with rare gases). 2) Polarization methods have been developed to study alignment of J states, based on rapid modulation (75 kHz) of a single mode diode laser, and used to study collisional alignment of CO_2 in supersonic jets. 3) High resolution flash kinetic spectroscopy has been used to investigate reaction kinetics of OH radical with hydrocarbons, as well as to obtain absolute quantum yields for photofragmentation of HNO_3 and H_2O_2 at 193 nm and 248 nm. 4) Pressure broadening rates of OH radical relevant to IR "airglow" detection and characterization have been measured. 5) A new capability has been developed for measuring state-resolved energy transfer in "hot atom" collisions of open shell radicals. By absolute absorbance measurements and analysis of high resolution Doppler profiles, both integral and differential cross sections to a specific final J state are obtained for Cl + HCl scattering.

14. SUBJECT TERMS

infrared airglow; energy transfer; potential energy surfaces; Dopplerimetry

15. NUMBER OF PAGES

17

16. PRICE CODE

17. SECURITY CLASSIFICATION OF REPORT	18. SECURITY CLASSIFICATION OF THIS PAGE	19. SECURITY CLASSIFICATION OF ABSTRACT	20. LIMITATION OF ABSTRACT
unclassified	unclassified	unclassified	

NSN 7540-01-280-5500

DTIC QUALITY INSPECTED 1

Standard Form 298 (Rev. 2-89) Prescribed by ANSI Std. Z39-18 298-102

94 3 22 037

Abstract:

Achievements under the AFOSR grant have been in the following areas 1) We have developed a new method for state-to-state collisional energy transfer in crossed molecular beams, based on high sensitivity direct IR laser absorption, and allowing absolute cross sections to be obtained by measurement of absolute number densities of the scattering species (CH_4, H_2O, HF with rare gases). 2) Polarization methods have been developed to study alignment of J states, based on rapid modulation (75 kHz) of a single mode diode laser, and used to study collisional alignment of CO_2 in supersonic jets. 3) High resolution flash kinetic spectroscopy has been used to investigate reaction kinetics of OH radical with hydrocarbons, as well as to obtain absolute quantum yields for photofragmentation of HNO_3 and H_2O_2 at 193 nm and 248 nm. 4) Pressure broadening rates of OH radical relevant to IR "airglow" detection and characterization have been measured. 5) A new capability has been developed for measuring state-resolved energy transfer in "hot atom" collisions of open shell radicals. By absolute absorbance measurements and analysis of high resolution Doppler profiles, both integral and differential cross sections to a specific final J state are obtained for Cl + HCl scattering.

Accession For
NTIS GRA&I ☑
DTIC TAB ☐
Unannounced ☐
Justification
By
Distribution/
Availability Codes
Dist | Avail and/or Special
A-1

Approved for public release; distribution unlimited.

SUMMARY OF RESEARCH ACCOMPLISHMENTS UNDER CURRENT AFOSR FUNDING (1990-1993)

The efforts over the present granting period have been in the following areas: i) to exploit the fully operational, high resolution flash kinetic spectrometer to probe transient kinetics, photofragmentation dynamics, and collisional broadening for OH radical, ii) to develop the capability for state-to-state collisional energy transfer in crossed molecular beams via high sensitivity, direct absorption of a single mode IR probe laser, iv) implement fast polarization modulation methods for detecting M_J alignment in rotational states via direct IR absorption, and v) develop high resolution IR laser Dopplerimetry methods for measuring velocity resolved Cl + HCl scattering in open shell collision systems. Some highlights of the past three years are briefly summarized below.

A. State-to-state Collisional Energy Transfer in Crossed Supersonic Expansions

As a major thrust of this current granting period, we have developed a high resolution IR method of monitoring state-to-state collisional energy transfer in low density, crossed supersonic jets. The method involves i) supersonic cooling of the IR absorber into a well defined initial rotational state, ii) scattering from this state into various final states by collisions with a second supersonic jet, and iii) probing the final state distribution by fractional absorption of the F-center or diode laser light in the intersection region of the two expansions. By virtue of dual beam subtraction and near shot noise limited absorption methods, the IR detection sensitivity ($\lesssim 10^{-6}/\sqrt{Hz}$) is sufficiently high to observe collisionally excited species present at the very low densities needed to ensure single inelastic collision conditions. As result of the small IR Doppler widths and intrinsically high resolution of the IR probe laser, the method offers better than 0.01 cm^{-1} resolution of the final scattering states. This reflects more than <u>three orders</u> of magnitude improvement over current time-of-flight methods that probe kinetic energy loss distributions in the scattered flux. One of the clear advantages of such an IR based technique is its general applicability to a nearly unlimited choice of collision systems. This capability is of particular importance to IR "airglow" phenomena, and opens up for detailed study many atmospherically relevant IR emitters such as CH_4, H_2O, CO_2, O_3, N_2O, etc. which are inaccessible to more sensitive LIF and MPI optical methods.

One configuration of the crossed jet apparatus is schematically shown in Fig. 1. Two pulsed valves are positioned at right angles to the tunable F-center probe laser, which is multipassed up to 36 times in a polarization preserving Herriot cell. Typical distances from the jet to intersection

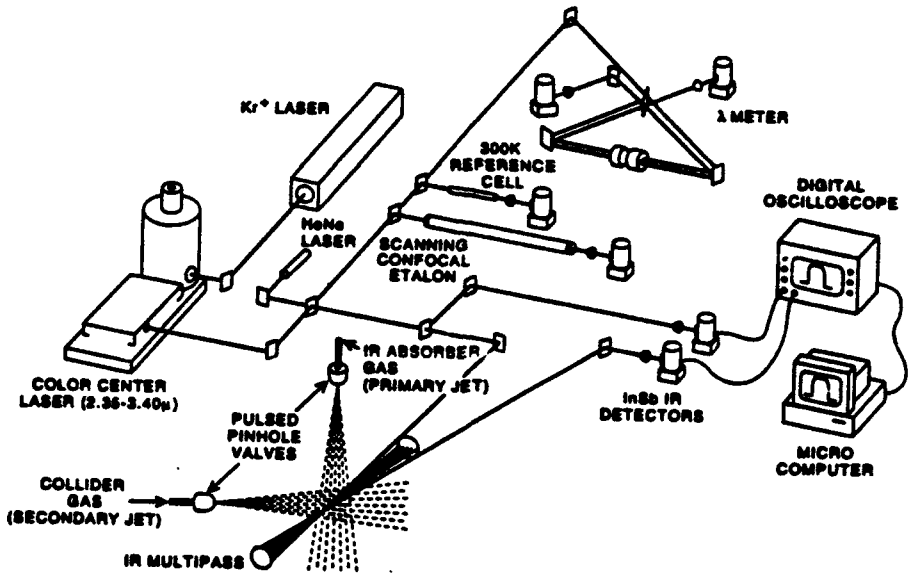

Fig. 1. Schematic of the current crossed jet apparatus for state-resolved energy transfer

region are 10-15 cm, with target densities on the order of $10^{11}/cm^3$, and collider densities between $0\text{-}5\times10^{12}/cm^3$, respectively. High resolution scans over individual Doppler broadened transitions are performed, and the scattered state density integrated the over all final velocities. In order to ensure single inelastic collision conditions, the final state signals are monitored as a function of the stagnation pressure behind the second jet, and which demonstrate a linear dependence on collision density over the range of stagnation pressures included in the analysis.

We have performed a series of state-resolved scattering studies for CH_4 colliding with Ar, Ne and He, and have initiated parallel studies on the corresponding HF and H_2O + rare gas systems as well. The CH_4 scattering target offers a particularly novel advantage, since due to nuclear spin ($I_H=1/2$) statistics the molecules cool down into the lowest energy level of the three distinct symmetry species (see Fig. 2), which are not interconverted by collisions in the intersection region. Consequently, one is able to perform three scattering experiments simultaneously, out of the A ($J''=0$), F ($J''=1$) and E ($J''=2$) rotational symmetry manifolds of CH_4. A similar advantage is obviously offered in any system with symmetrical, non-zero spin nuclei, e.g. H_2O, NH_3, CF_4, etc.

Sample data for CH_4 scattered from $J''=0(A_1)$ into $J'=3(A_2)$, $4(A_1)$, and $6(A_2$ and $A_1)$ by collisions with He (E_{coll} = 460 cm^{-1}) are shown in Fig. 3(a,b), and verify the anticipated linear

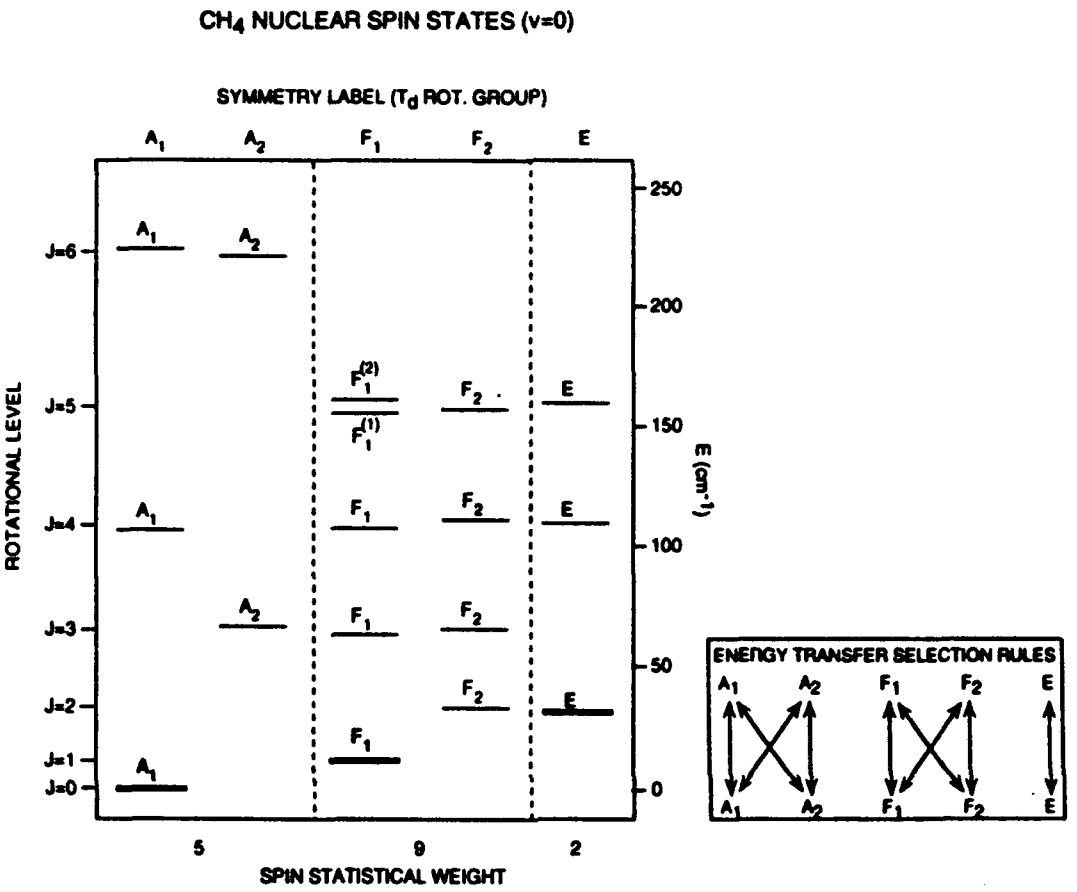

Fig. 2. Relevant nuclear spin symmetries (A,E, F) and collisional pathways for the CH_4 rotational manifold.

dependence on backing pressure. Relative state-to-state collision cross sections are readily obtained from the slope ratios for the various curves. However, one major advantage of a high resolution IR probe technique is that absolute number densities in the scattering region can be easily determined from the fractional absorbances and known IR line strengths. Specifically, by "doping" the scattering beam with trace amounts of an IR absorber, the column integrated scattering densities (integrated over the multipass region) can be reliably determined. With a dual, skimmed beam geometry to better define initial collision velocities in the intersection region, the apparatus will also be able to measure differential state-to-state cross sections as well via high resolution Dopplerimetry on the scattered species. It is worth noting that at this level of quantum state detail in CH_4, many of the simple quantum and energy gap "law" predictions are strongly violated. For example, the $j=3 \leftarrow 0$ (A symmetry) cross section is almost three times as large as the $j=3 \leftarrow 1$ (F symmetry) cross section, despite both a smaller energy and quantum "gap."

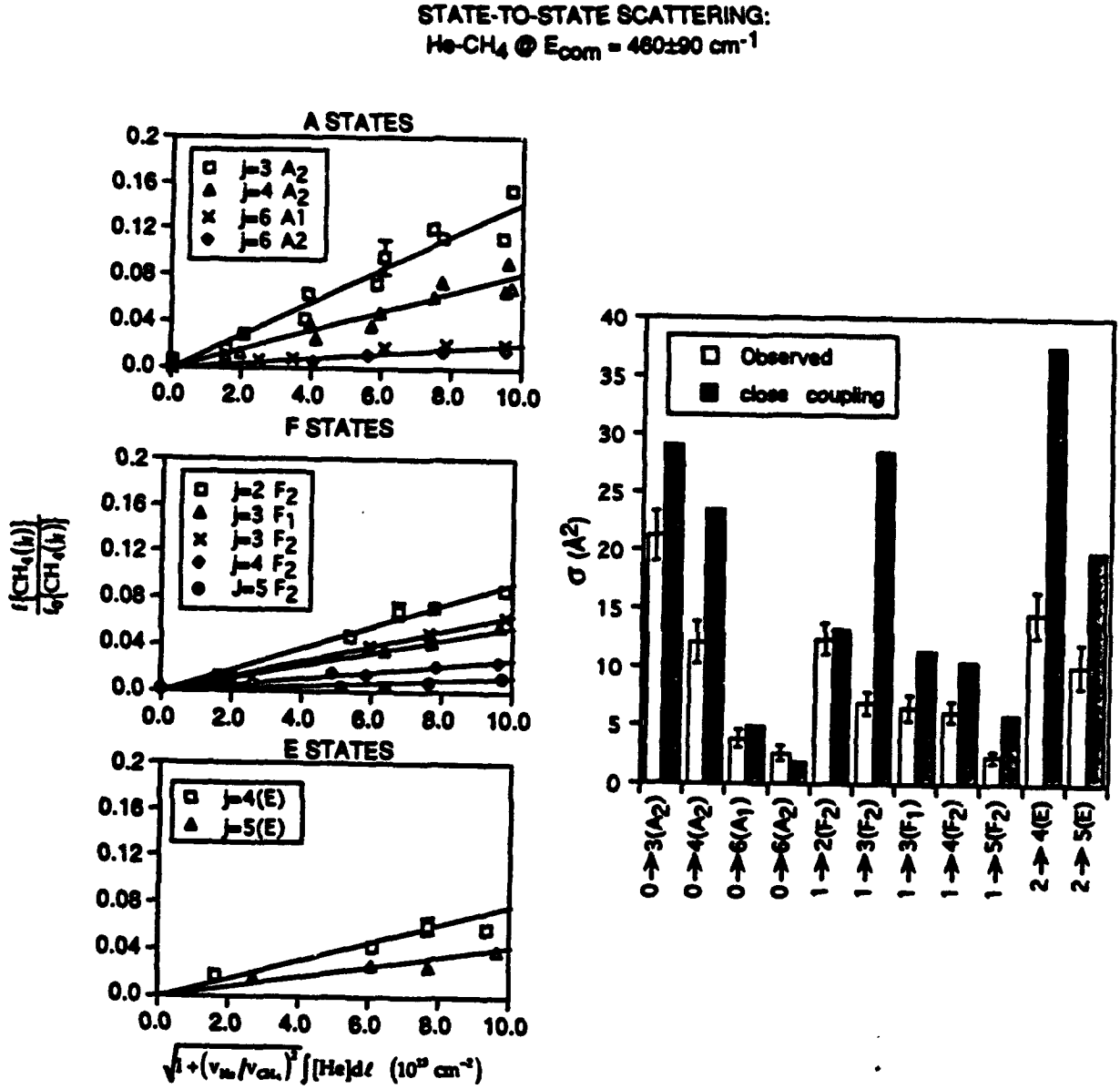

Fig. 3. Sample data for He + CH_4 scattering at E_{com} = 460 cm^{-1}

As one additional example, inelastic scattering data for Ar + H_2O out of the lowest "para" ($J_{K_aK_c} = 0_{00}$) and "ortho" ($J_{K_aK_c} = 1_{01}$) levels are shown in Fig 4. The plot indicates the total loss of the initial quantum state (column integrated densities) as a function of stagnation pressure of the scattering rare gas. Note the factor of 3 difference in the initial populations due to the 3:1 nuclear spin statistics in H_2O.

We have purposefully chosen relatively "simple" collision systems for initial investigation, in order to facilitate the most rigorous connection between the experimental data and a theoretical description of the dynamics. In collaboration with Prof. Jeremy Hutson from the University of Durham, we therefore have extended full QM scattering codes to include both i) atom + spherical top and ii) atom + diatomic collision partners. From the T_d symmetry of CH_4, the lowest order form of the potential can be written as an radially dependent expansion in linear combinations of spherical harmonics, i.e.

$$V(R,\chi,\theta) = V_0(R) + V_3(R)\cdot T_3(\theta,\chi) + V_4(R)\cdot T_4(\theta,\chi) + \ldots \qquad (3)$$

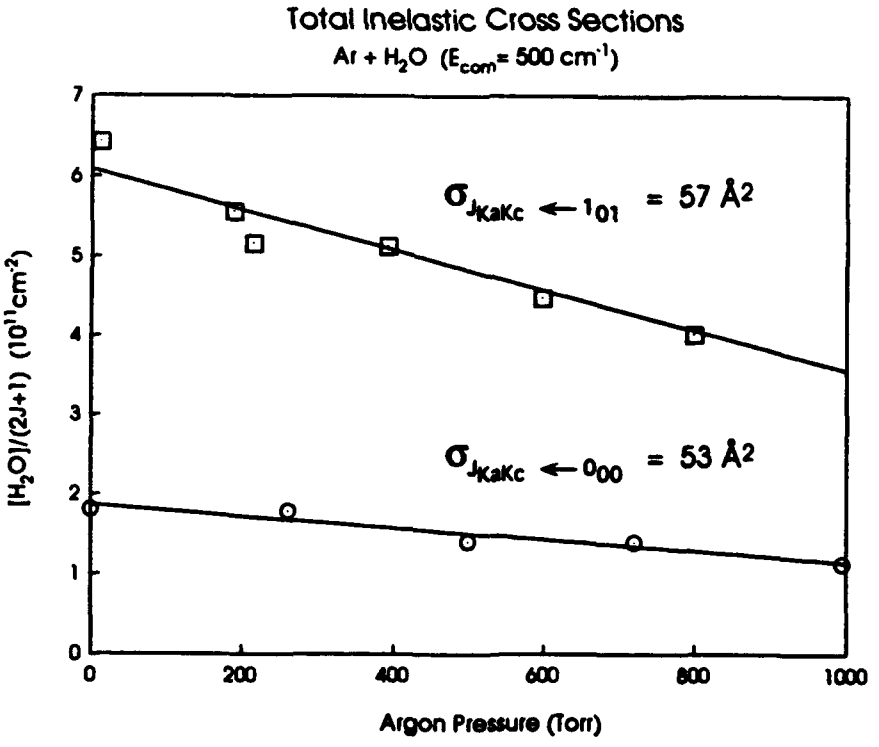

Fig. 4. Ar + H_2O scattering at E_{com} = 500 cm^{-1}. The ⊡ and ⊙ represent total loss out of the 1_{01} (ortho) and 0_{00} (para) levels of water, respectively.

The predicted state-to-state cross sections can then be obtained from a trial form of the potential by both approximate coupled states and full close coupling calculations. The previous analysis by Secrest of the time-of-flight scattering data was able to infer the lowest order V_3 anisotropy in the He + CH_4 potential. Full close coupling calculations on this potential are in rough qualitative agreement with the present scattering results, but indicate considerable discrepancies, particularly in the J dependent trends for a given nucelar spin symmetry and for the higher ΔJ collisions. These higher ΔJ cross sections contain detailed information on V_4 and higher order anisotropies, which we are currently using to refine the CH_4-rare gas intermolecular potentials. In particular, we find that the ratio of V_3 to V_4 terms controls dramatically influences the relative cross sections into the various fine structure levels, quantities that are directly measured in the experimental data.

B. IR Polarization Studies of Rotational M_J Alignment

The high spectral resolution in the above apparatus permits cross sections for J-state changing collisions to be studied in considerable detail. An even finer probe of the anisotropy in the intermolecular potential can be obtained from studies of the simultaneous M_J-state changing collisions. In an anisotropic velocity field such as exists in a crossed beam, these processes can result in a macroscopic alignment of the overall final state rotation by a single inelastic collision, and can be studied via polarization dependent absorption methods. In the course of the next granting period, we will implement such polarization modulation methods in the crossed beam geometry, and thereby probe the final $|J, M_J>$ state distributions via the infrared "birefringence" of the scattered molecules. In addition to providing a more state-to-state description of collision dynamics, these anisotropic scattering processes may provide a novel source of highly aligned states for further studies of stereospecific collision and chemical reaction phenomena.

As a necessary initial experiment, we have used high resolution IR diode lasers to investigate the collisional formation of aligned J states induced simply by relative velocity slip in a seeded supersonic expansion. The present experimental method (see Fig. 5) involves i) fast, amplitude preserving modulation of the probe IR laser polarization with an 80 kHz photoelastic ZnSe crystal, ii) polarization dependent attenuation of the probe light by molecules in the jet, followed by iii) phase sensitive detection of this modulation on the transmitted light. Our test system has been CO_2 expanded in H_2, He and Ar diluent, taking advantage of the strong ν_3 absorption band at 4.3 μm, a single mode laser diode which conveniently accesses this band, and the relative simplicity of quantum calculations for "ball + stick" collisional scattering. Furthermore, natural abundance CO_2 has zero spin nuclei,

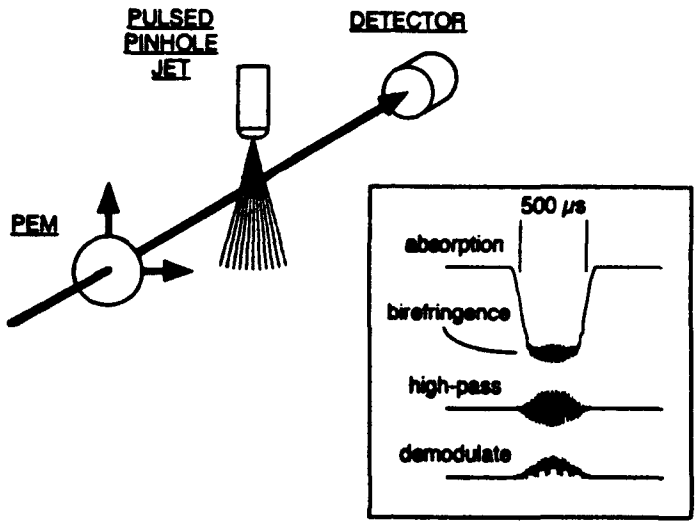

Fig. 5. Apparatus schematic for measuring rotational alignments

and hence dipolar couplings between $\underset{\sim}{J}$ and $\underset{\sim}{I}$, which can cause $\underset{\sim}{J}$ to precess in the lab frame, vanish identically. Experimentally we directly measure the polarizance, i.e.

$$P = \frac{A_{\perp} - A_{\parallel}}{A_{\perp} + A_{\parallel}} \tag{4}$$

where $A_{\perp}$ and $A_{\parallel}$ are the measured absorbances for light polarized perpendicular and parallel to the expansion axis, respectively. This polarizance can be directly related to the alignment parameter via

$$A_0 = \frac{4P}{3-P} \cdot \frac{1}{h^{(2)}(J',J'')} \tag{5}$$

where $h^{(2)}$ is a function only of the upper/lower states of the probe transition. This alignment parameter is conventionally used to determine the second moment of an M_J distribution in $P_t(\cos\theta)$. The first moment of such a distribution corresponds to rotational orientation, and can be obtained from analogous measurements with modulated, circularly polarized light. With the present modulated absorption method, we have demonstrated a sensitivity to fractional polarizance in the jet samples of $\lesssim 0.1\%$.

A sample set of data (J=0,2,4) for 6.4% CO_2 in He at 700 Torr is shown in Fig. 6. As expected, there is a null alignment signal for J=0, which serves as an essential diagnostic at these

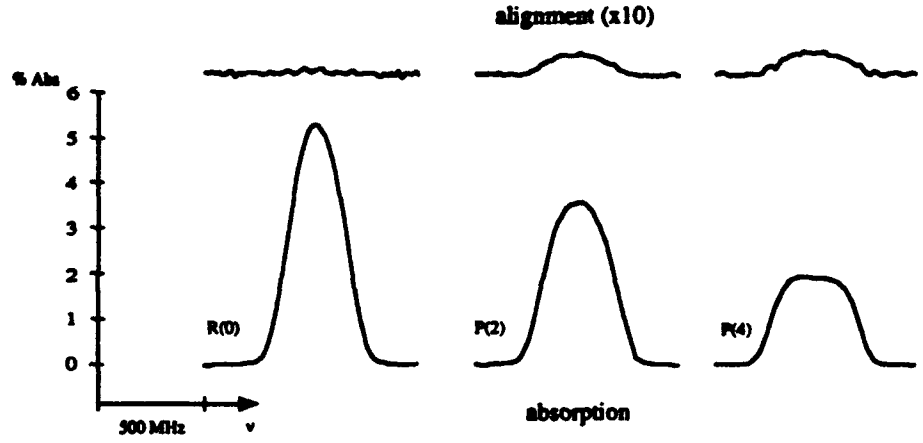

Fig. 6. Typical alignment scans over CO_2 transitions (ν_3 asymmetric stretch)

high sensitivity levels for stray birefringence, optical feedback to the diode laser, etc. For any $J > 0$, however, there are quite significant alignment signals that increase monotonically with J to a asymptotic maximum value ($A_0 \approx -0.10$) by $J=8$, corresponding to a roughly 3:2 enhancement of the low $|M_J|$ levels over that of an isotropic distribution. A similar asymptotic trend in J was also observed by Bergmann and coworkers in Na_2 expansions. This alignment is negative, which is consistent with an excess of CO_2 molecules rotating with J perpendicular to the expansion axis. By virtue of the relative velocity slip, the alignment signals are also sensitive to the mass of the expansion gas, dropping by 5 fold between He and Ar. However, despite the $\sqrt{2}$ greater relative velocity slip, we observe a 2-fold reduction in CO_2 alignment signals in H_2 vs. He expansions. This suggests a higher efficiency for M_J scrambling collisions with structured vs. unstructured diluent gases, in contrast to the results of Friedrich et al. for I_2/He and I_2/H_2 expansions. Interestingly, the maximum alignment values are in good agreement with the predictions from a steady state classical model developed by Zare and coworkers, taking eccentricity parameters from the recent He + CO_2 intermolecular potential by Beneventi et al. Considering that CO_2 has a relatively small eccentricity, it seems quite probable that even more highly aligned molecular samples would be experimentally accessible in the IR for more "rod-like" species such as cumulated acetylenes. Furthermore, this magnitude of alignment for CO_2 develops for even modest backing pressures of He (i.e. 200-1000 Torr), and thus it is also quite probable that many supersonic jet pinhole experiments are being performed, quite unintentionally, on non-isotropic molecular samples. Interestingly, however, we have observed no measurable alignments on species to date in a slit expansion geometry.

C. Absolute OH Photolysis Quantum Yields

The production of OH via photolysis of HNO_3 and H_2O_2 has received considerable attention in recent years due to its importance as a precursor for laboratory studies of open shell van der Waals complexes, vibrationally mediated photodissociation, inelastic energy transfer and reactive kinetics, with additional interest in HNO_3 as a stratospheric source of OH from unfiltered solar photolysis in the 190-220 nm region. Nevertheless, absolute quantum yields for these photolytic processes have been quite difficult to determine, due primarily to the difficulty in establishing a reliable probe of absolute OH radical concentrations. Consequently, most studies have been based on relative measurements, calibrated against standard reference systems such as H_2O_2 photolysis at 248 nm.

With a reliable dipole moment function for OH experimentally measured ($0.70\ \text{Å} \leq R \leq 1.76\ \text{Å}$) from the prior work of Nelson et al. in our laboratories, the integrated absorption cross sections for OH (v'←v") vibrational transitions have been determined as a function of J", ΔJ, and F=1 or 2 spin orbit states. From a high resolution scan over the spectral line profile, therefore, absolute OH concentrations in a given quantum state can be measured actinometrically in the flash kinetic spectrometer from the absorbance of the narrow band IR laser in a known path length. By repeated measurements over the range of thermalized OH quantum states, both the equilibrium nature of the distribution and the total density of $[OH]_{tot}$ can be determined. From additional measurements on the spatial profile and homogeneity of the excimer beam, one can also simply obtain the concentration of absorbed UV photons, i.e. $[\text{UV photons}]_{abs}$. The ratio of these two quantities provides an absolute measure of the quantum yield, i.e.

$$\Phi = [OH]_{tot}/[\text{UV photons}]_{abs} \qquad (6)$$

With this direct method, we have performed absolute quantum yield measurements for HNO_3 and H_2O_2 at 193 nm and 248 nm, and find each quantum yield to be less than 100% photon efficient (see Table I). This includes photolysis of H_2O_2 at 248 nm, for which a quantum yield of 2.0 (i.e. unit

Table I. Photolysis Quantum Yields

Wavelength	Precursor	Φ
193 nm	HNO_3	0.47±0.06
248 nm	HNO_3	0.75±0.10
193 nm	H_2O_2	1.22±0.13
248 nm	H_2O_2	1.58±0.23

efficiency for breaking the O-O bond) has often been used as the reference system in many relative measurements. The HNO_3 system at 193 nm is particularly dramatic, with the production of OH actually constituting less than half ($42 \pm 6\%$) of all contributing photolysis channels. A sample data plot for 193 nm is shown in Fig. 7, with the dashed line corresponding to a 100% photodissociation quantum yield shown for comparison. The presence of significant non-OH producing channels in HNO_3 photolysis has since been confirmed by Curl and coworkers, (via HONO production), and Lee and coworkers (via O atom production). The presence of $O(^3P)$, $O(^1D)$ and $H(^2S)$ channels in HNO_3 photolysis has been recently quantified from resonance fluorescence studies by Ravishankara and coworkers.

E. Collisional Line Broadening in OH (v=1←0) Transitions

There has been a considerable interest in developing accurate intermolecular potentials for open shell systems. A particular focus has been the Ar-OH complex, for which a high level ab initio potential presently exists and the electronically excited potential surface has been extensively investigated. The corresponding ground state potential has proven more difficult to probe, although there have been some very challenging SEP and IR-UV double resonance studies by Lester and

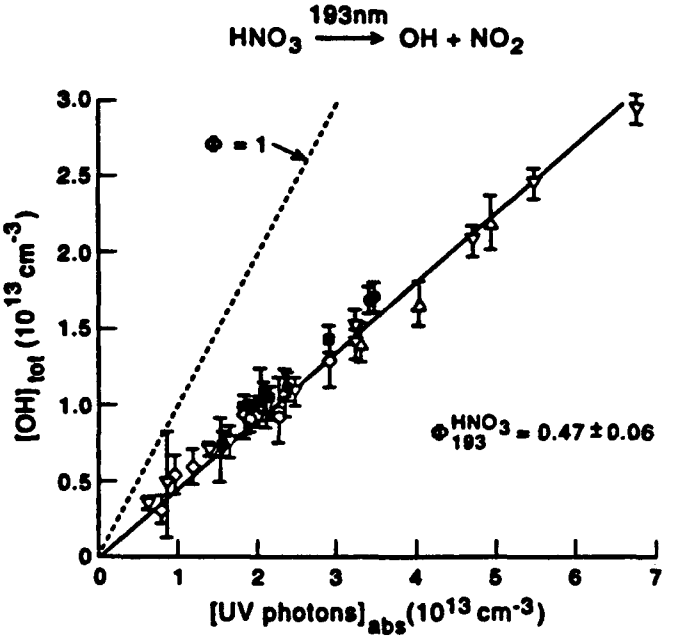

Fig. 7. Sample data plot for determining the quantum yield for OH production from HNO_3 photolysis at 193 nm.

coworkers. Alternative, non-spectroscopic tests of this ab initio Ar + OH potential for the ground state would be quite useful, as well as for the more complex systems such as N_2 + OH and O_2 + OH which are of more direct relevance to airglow phenomena.

We have therefore investigated collisional broadening on the v=1←0 transition for X($^2\Pi$) OH radicals in the presence of He, Ar, N_2, and O_2. This flows naturally from the above photolysis quantum yield studies, since high resolution scans over individual transitions of the transient OH radical are necessary in order to obtain the integrated absorbances. The high resolution spectral data are analyzed both as i) a Voigt convolution over Gaussian (thermal) and Lorentzian (collisional broadening) contributions and ii) a Dicke narrowed line shape, as a function of buffer gas pressure, end-over-end rotational angular momentum (N), spin orbit (F=1,2), and lambda doublet (±) state for each of the four buffer gases.

A sample presentation of the pressure broadening results is shown in Fig. 8 for the P(2.5)1' transition, which demonstrates an ordering (i.e. $k^{N_2} > k^{O_2} > k^{Ar} > k^{He}$) that is consistent with well depths for the corresponding N_2, O_2, Ar and He complexes with HF. The complete set of results as a function of N reveals several interesting trends. i) The pressure broadening is strongly rotational state dependent, decreasing with increasing N. This is consistent with a similar J dependence in pressure

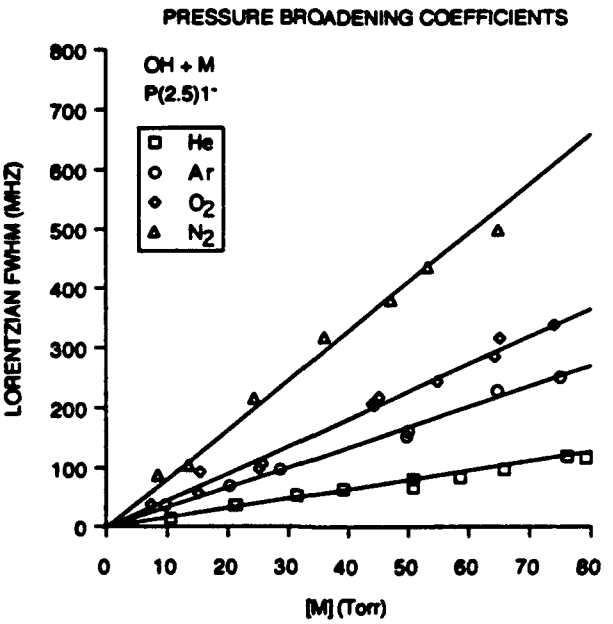

Fig. 8. Pressure broadening results for the P(2.5)1' transition in OH(v=1←0) in the presence of N_2, O_2, Ar and He buffer gas

broadening rates observed in the HF + Ar and Ne systems, and would support a metastability of high rotational levels of OH to collisional relaxation. ii) With the exception of He + OH, the pressure broadening rates depend only to the end-over-end angular momentum, N, and within experimental error are insensitive to either spin orbit or lambda doublet state. It is interesting to note that this issue of lambda doublet propensities has relevance in interstellar dynamics, since some models for population inversions in the OH maser require unequal cross sections for collisional excitation into the two components. iii) In addition to the pressure broadening, we have observed and analyzed collisional IR Dicke narrowing for the first time in an open shell hydride (Ar + OH). We are presently collaborating with Dr. Sheldon Greene to predict the J-dependent line broadening and narrowing effects from open shell quantum scattering calculations, and thereby independently test the accuracy of the ab initio Ar + OH ground state potential energy surface.

E. Flash Kinetic Spectroscopy of Cl Radical Reactions

The steady state concentrations of ozone destroying Cl radicals in the stratosphere is strongly linked to the removal rates by reaction with hydrocarbons, i.e.

$$Cl + RH \rightarrow HCl(v) + R \qquad (7)$$

where RH has been generated at the earth's surface and survives propagation upward through the atmosphere. The predominant hydrocarbon species at these altitudes is methane (1 ppm) with larger, non-methane hydrocarbons at 3-4 orders of magnitude lower concentrations (0.1-1 ppb). The rates for Cl + non-methane hydrocarbons, however, are more than 3 orders of magnitude faster than for Cl + CH_4, and hence these larger hydrocarbon species can also contribute to the removal of Cl radical.

We have used the IR flash kinetic spectrometer to investigate the absolute rates of these reactions via production of HCl. The Cl atoms are formed by excimer laser photolysis of CCl_4 or $CFCl_3$, thermalized by excess buffer gas, and the rate of hydrogen abstraction probed by monitoring the time resolved, single exponential appearance of the HCl(v=0) product under fully rotationally and vibrationally relaxed conditions. The results for the series of C_1-C_4 hydrocarbons are shown in Table II. The observed rates for Cl + CH_4 agree quantitatively with a wide range of previous studies, and

Table II. Cl + RH rates (10^{-11} cm^3/molecule/sec)

RH	$k_{observed}$	$k_{modeling}$ [a]
methane	0.0105(4)	0.0104
ethane	4.42(26)	5.7
propane	9.08(52)	16
isobutane	9.66(31)	14
n-butane	13.3(10)	21

[a] from a recent compilation by W. B. Demore et al.

in particular supports the value used in current atmospheric models. However, the present work indicate significantly slower H abstraction rates for the C_2-C_4 species, with as much as 30%-70% discrepancies from previous measurements. These measurements have been tested extensively i) over 2 orders of magnitude in buffer gas pressures, ii) over 1-2 orders of magnitude in [Cl]/[RH] ratios, iii) for a range of buffer gases to quench any vibrationally excited states, and iv) for several thermally populated J states of HCl. Due to the relevance of these reactions in current atmospheric models, these results are rather surprising and are providing a stimulus for reinvestigation of these systems via alternative techniques. The discrepancy for Cl + ethane (see Fig. 9) is of particular concern due to its use as reference system in relative reaction rate measurements.

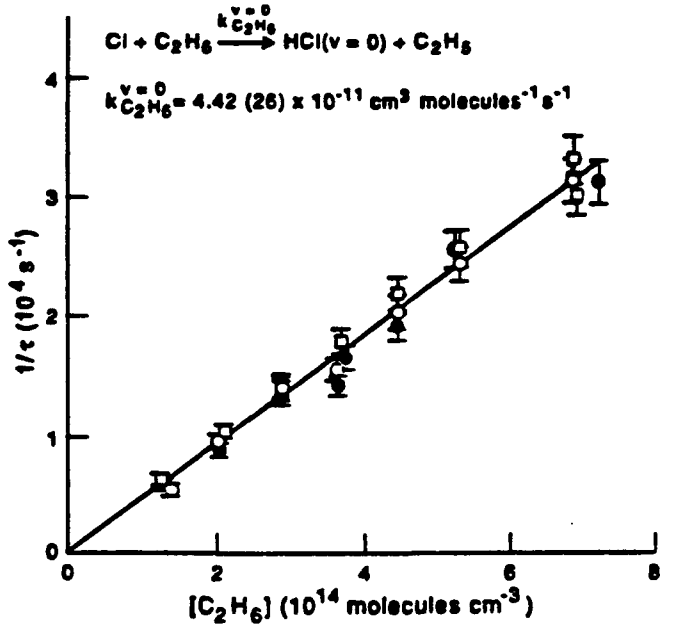

Fig. 9. Stern-Volmer plot for H atom abstraction of ethane by Cl radicals

F. Velocity resolved scattering in open shell (Cl + HCl) collision via high resolution IR laser Dopplerimetry

As a recent thrust of the flash kinetic spectrometer, we have been investigating energy transfer in "hot atom" collisions, using the high resolution IR laser to probe both i) the final quantum states and ii) the final velocity distributions. The initial system we have studied is Cl + HCl, monitoring the HCl ($v=1\leftarrow0$) transition on a series of R branch transitions up to J = 12. The Cl atoms are prepared by excimer laser photolysis of Cl_2 molecules at 308 nm, which generates a Cl atom velocity of $\approx$2000 m/s. If one includes the relative motion of the initial Cl_2 and HCl species, this translates into a center of mass collision energy for Cl + HCl of $E_{cm} \sim 3500$ cm^{-1}, sufficient to surmount the 3000 cm^{-1} activation barrier to Cl-H-Cl, H atom exchange (see Fig. 10). Although the reactive component is still relatively small at these energies, the collisions significantly sample "frustrated" reactive attempts, and thus state resolved energy transfer can probe the entrance and exit channels to reaction.

By measuring absolute absorbances, and integrating over the velocity profile, we have measured the net integral cross sections for collisional excitation into a given final state J from a room temperature distribution ($<J_{initial}>_{300K} \approx 3$) in the flow cell. The results are summarized in Fig. 11, and demonstrate a monotonic decrease in cross section with increasing J. In particular, the maximum J excited is 12, far from J=18 accessible at these center of mass collision energies. The

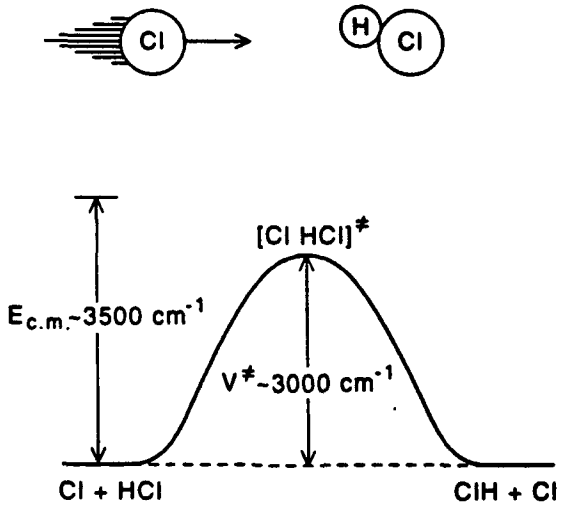

Fig. 10. Schematic of the Cl + HCl collision system for state-resolved energy transfer on open shell potential surfaces

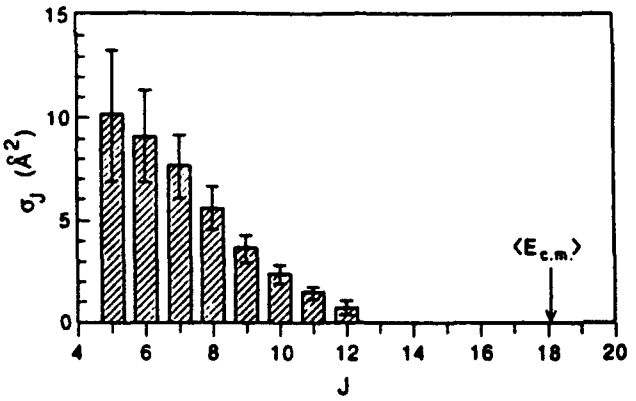

Fig. 11. Absolute integral cross sections (in Å^2) for scattering of thermal HCl into a final J level

inefficiency of this hot atom energy transfer process is not due to angular momentum constraints, but instead is a reflection of non-colinear "heavy-light-heavy" collision dynamics. In essence, optimum collision geometries for rotational energy transfer require the incident Cl atom to interact most strongly with the H end of HCl, which does not effectively slow the Cl atom in the Cl-HCl center of mass frame.

Such a heavy-light-heavy collision model would predict strongly forward scattering of the Cl atom, which we have investigated via time resolved high resolution Dopplerimetry on the recoiling HCl quantum states. In order to implement these ideas, we have developed Green's function methods for analyzing the Doppler profiles in the single collision regime, and thereby extracting absolute state-to-state differential cross sections into a given final HCl J state. The results are shown in Fig 12, and clearly demonstrate the anticipated trend toward strongly backward scattered (i.e. $\cos(\Theta) \approx -1$) HCl product. We are currently investigating trajectory calculations on a state-of-the-art Cl-H-Cl surface to compare with both the integral and differential cross section results, as well as to verify the key elements of the collision dynamics.

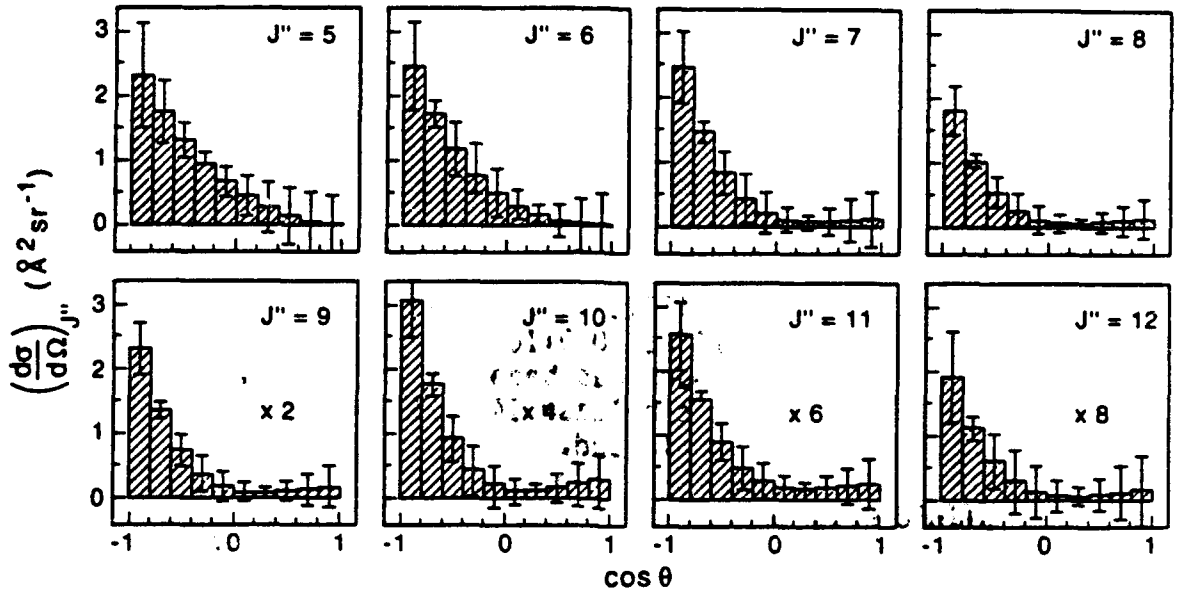

Fig. 12. Absolute differential cross sections (in Å^2/steradian) for scattering of thermal HCl into a final J" level. Note the strong propensity for cos(θ) = -1, i.e. predominantly forward scattering of the Cl atoms in the center-of-mass frame